의학박사 학위논문

상염색체우성 다낭신질환에서 뇌동맥류의 발생기전 규명을 위한 다낭성 신장 적출 조직 단백체 분석 연구

Exploring the Molecular Pathways of Intracranial Aneurysm Formation in Autosomal Dominant Polycystic Kidney Disease using Proteomic Analysis

울산대학교대학원

의학과

김 진 명

상염색체우성 다낭신질환에서 뇌동맥류의 발생기전 규명을 위한 다낭성 신장 적출 조직 단백체 분석 연구

지도교수 신 성

이 논문을 의학박사 학위 논문으로 제출함

2024 년 8 월

울 산 대 학 교 대 학 원

의 학 과

김 진 명

김진명의 의학박사 학위 논문을 인준함

심사위원장 이 세 원 인

심사위원 신 성 인

심사위원 황 상 현 인

심사위원 권 현 욱 인

심사위원 전 흥 만 인

울 산 대 학 교 대 학 원

2024 년 8 월

ABSTRACT

Introduction: Intracranial aneurysm (IA) frequently coincides with autosomal dominant polycystic kidney disease (ADPKD), exhibiting incidence rates nearly 10 times higher than the general population. However, the exact mechanism of how these two conditions are related remains unclear. This study aims to identify mechanisms behind IA occurrence in ADPKD patients using proteomics and to discover potential protein biomarkers for early diagnosis.

Method: Pre-kidney transplantation ADPKD patients underwent cranial CT and/or MR angiography, with findings dictating assignment to either a control group (ADPKD without IA, n=20) or IA group (ADPKD with IA, n=9). During transplantation, bilateral nephrectomy was performed and native renal arteries were sampled for proteomic analysis via a liquid chromatography-tandem mass spectrometry. Differentially expressed proteins were subjected to bioinformatic analysis and a protein-protein interaction network analysis.

Results: Eight proteins showed significant variation between IA and control groups, with four proteins upregulated (DIS3, MMS19, EXOC8, RAB6A) and four downregulated (CLUH, SYNC, MEF2D, WDR36) in IA group (Log_2 fold change (FC) >2 and false discovery rate [FDR] q-value <0.05) compared to the control group. These proteins correlated with pathways implicated in IA development, such as ciliopathy, exocytosis, inflammation, extracellular matrix remodelling, and apoptosis. These proteins were quantitatively validated using immunoblot and found to be consistent with proteomic data. Moreover, a connection was observed between protein expression and clinical metrics (bilirubin, prothrombin time, platelet count), indicating their potential as early diagnostic markers.

Conclusion: This study is the first to employ renal artery samples to study underlying mechanisms for IA in ADPKD patients by proteomics. We identified and validated novel candidate markers that are either upregulated or downregulated in the IA group compared to the control group. This research's finding opens new avenues for understanding and diagnosing IA in ADPKD, potentially leading to earlier diagnosis and targeted treatments.

Contents

List of Tables and Figures

1. INTRODUCTION

Autosomal dominant polycystic kidney disease (ADPKD) is the most frequent form of hereditary renal disease affecting 1 in 1000 people and characterized by gradual and irreversible decline in renal function while accounting for 10% of cases of the kidney failure[1-3]. Apart from renal manifestations, changes in other organs may be present, including liver cysts and intracranial aneurysms. Intracranial aneurysms are a rare vascular manifestation, affecting only 5%–9% of the general population. However, they are substantially more prevalent among ADPKD patients, who experience a three- to five-fold higher incidence rate, with prevalence rates climbing up to 40%[4-6].

Although numerous publications have reported a clear association between ADPKD and the occurrence of intracranial aneurysms, there is a lack of data available to define the underlying mechanism for this manifestation. Although few studies included a large population (>1000), many focused on identifying risk factors for developing intracranial aneurysms or indications for screening for this disease in ADPKD patients[7-9] . Because of high mortality and morbidity associated with intracranial aneurysms, it is critical to diagnose early at its developing stage and treat before fatal events occur such as rupturing of aneurysms. Understanding the mechanism behind the development of intracranial aneurysms can lead to early diagnosis and treatment, significantly improving outcomes for ADPKD patients.

There have been several speculations on mechanisms behind IA in ADPKD patients. Vascular remodeling due to a mounting inflammation response which is evidenced in remarkable inflammatory markers, endothelial dysfunction[10]. Yet, there is a still lack of knowledge of the mechanisms underlying formation, progression and frequent occurrences of IAs in ADPKD patients, which hinder the development of effective therapies and clinical approaches for diseased patients.

An evaluation of changes in the peptidome and/or proteome may provide information of pathophysiologic and clinical significance and enable the development of future diagnostic or prognostic tools. However, before proteome or peptidome markers become clinically useful, the proteome itself must be thoroughly characterized in a process of intense multi-

stage research comparing different sample processing and analysis experimental laboratory settings. Our research focused on characterizing the proteome of vessels acquired from ADPKD patients with intracranial aneurysms using a bottom-up proteomic methodology.

To date, no discernible genetic or protein variations have been detected in extensive depth between ADPKD patients with IA and without IA. This lack of definitive biomarkers has hindered the development of effective screening protocols for intracranial aneurysms in ADPKD patients and the prompt management of the disease prior to the onset of complications. As a result, early diagnosis and timely intervention to prevent potentially life-threatening complications remain challenging for clinicians.

This investigation aimed to identify protein variations in renal artery samples from different groups of ADPKD patients, specifically those with IA and those without IA. The primary objective of this study is to uncover potential underlying mechanisms for IA formation in individuals with ADPKD by identifying differentially expressed proteins using proteomics. The results may provide valuable insights that could aid in monitoring IA development and facilitate early intervention for ADPKD patients.

2. MATERIALS AND METHODS

2.1 Patients and sample collection

The present study was conducted following the guidelines of the Declaration of Helsinki and with the approval of the Research Ethics Committee at Asan Medical Center. All patients or their legal representatives provided written informed consent before participating in the study. Renal artery samples were collected from a total of 29 individuals from ADPKD patients who underwent kidney transplantation with concomitant bilateral nephrectomy between December 2018 and June 2022. The identification of ADPKD was established through the detection of five or more cysts in both kidneys via imaging, in combination with the presence of a familial history and comorbidities, once alternative cystic kidney disorders had been ruled out [11].

At our institution, brain magnetic resonance angiography (MRA) or computed tomography angiography (CTA) are routinely performed on all polycystic kidney disease (PCKD) patients who are scheduled to undergo kidney transplantation. Patients who were found to have no aneurysm during the screening were included in the control group. The IA group included patients who were identified as having aneurysms during screening and underwent preoperative interventions like coiling or embolization, as well as those who did not receive these treatments. The detection of intracranial aneurysms involved the identification of a bulging in the intracranial arterial wall measuring at least 1 mm in either CTA or MRA imaging studies [12]. The specimens were rapidly frozen using liquid nitrogen and kept at a temperature of -80°C.

2.2 Pre-operative diagnosis of ADPKD using imaging-based approach

At our center, we do not routinely use genetic testing to identify pathogenic mutations, such as PKD1 and PKD2, in patients with polycystic kidney disease before KT, primarily due to the complexity and cost involved. We conduct genetic tests for patients only when imaging results are inconclusive or in cases involving young individuals where the manifestations of the disease may not be fully evident. This approach maximizes the utility of genetic testing where it can offer the most significant benefit, helping to confirm the diagnosis of ADPKD when non-genetic diagnostic methods fall short. Although genetic testing can help predict the clinical course by identifying the genotype of patients, it is not mandatory to conduct genetic tests before KT solely to confirm ADPKD. Notably, ultrasound has proven to be highly effective in diagnosing ADPKD associated with PKD1 and PKD2 mutations, with an overall sensitivity, specificity, and accuracy of 97%, 100%, and 98%, respectively [13]. Moreover, when ultrasound findings are inconclusive, age-specific MRI criteria offer an additional diagnostic tool [14] . Specifically, the detection of more than 10 renal cysts in patients aged 16 to 40 years yields a 100% positive predictive value and sensitivity for ADPKD diagnosis[15].

To ensure we selected the right candidates for our research, we performed post-experiment analysis with serum samples from each patient via genetic testing. We collaborated with 3billion, Inc. in Seoul, South Korea (https://3billion.io/index), for expert

sample analysis and exome sequencing (method detailed in Supplemental data 1). Of the 29 patients, 20 samples were sent for testing, with the most common reason for exclusion being insufficient serum. Of these, 19 samples showed mutations in either PKD1 or PKD2, while one sample, which was negative for these mutations, displayed a single exon deletion suggesting further analysis with single-gene testing might be necessary. Despite not testing for PKD1 or PKD2 mutations in all samples, the majority of patients diagnosed with ADPCKD through imaging were confirmed by genetic testing, validating our imaging-based diagnostic approach in this study.

2.3 Clinical data collection

The medical records of all patients and controls were thoroughly examined in order to collect relevant data pertaining to various factors. Several parameters were examined, including age, gender, BMI, age at brain imaging study, presence of polycystic liver disease (PCLD), history of cerobrovascular accident (CVA), hypertension presence, diabetes mellitus (DM) presence and estimated Glomerular Filtration Rate (eGFR). Additionally, we gathered data on the angiographic findings of the aneurysm, including the number of aneurysms, their size (or the size of the largest aneurysm if multiple aneurysms were present), location, and type.

2.4 Sample preparation: Protein extraction, enzymatic digestion

In this investigation, renal arterial tissue samples were resolved in 400 μL of lysed buffer containing 5% SDS, 50 mM triethylammonium bicarbonate (pH 8.5) and 1× Halt™ protease inhibitor cocktail (Thermo Fisher Scientific) and homogenized with passed through a pestle (Kimble™ Kontes™ Pellet Pastle™, Thermo Fisher Scientific) 20 times. Protein extraction was applied by adaptive focused acoustics (AFA) technology (Covaris). The homogenized samples were transferred to the micro TUBE-500 AFA Fiber Screw-Cap (Covaris) and sonicated by S220 Focused-ultrasonicator (Covaris). Samples were subjected to AFA process using 175 peak power, 200 cycles per burst and 10 duty factor for 900 sec at 10 °C. Subsequently, the lysated samples were boiled at 80 °C using a heat block (MaXtable™ H10, Daihan Scientific, Korea) for 10 minutes and centrifuged at 18,000 ×g for 10 minutes at room temperature. We

transferred the supernatant fraction to the new lobind tube (Eppendorf). The protein concentration of each supernatant containing extracted proteins was measured with a BCA protein quantification kit (Pierce™ BCA Protein Assay Kit; cat. No.: 23225; Thermo Fisher Scientific, Waltham, MA, USA). A 300 µg aliquot of proteins was dissolved in 50 µL of lysis buffer and added dithiothreitol to a final concentration of 20 mM to the denatured sample, it was incubated at 95 °C for 10 min. The chemically reduced sample was then placed in iodoacetamide at a final concentration of 40 mM and reacted for 30 min at 25 °C in the dark. With a final concentration of 1.2% phosphoric acid, acidified samples were attached to suspension-trapping (S-Trap) mini columns (#CO2-mini-80, ProtiFi, Farmingdale, NY, USA). Following the manufacturer's protocol, we performed S-Trap proteolysis by adding 12 µg of Lys-C/trypsin mixture (#V5071, Promega, Madison, WI, USA) and incubating at 37 °C for 16 h. The digested peptide mixture was freeze-dried with a cold trap (CentriVap Cold Traps; Labconco, Kansas City, MO, USA) and stored at − 80 °C until use.

2.5 Liquid chromatography-tandem mass spectrometry

Peptide mixtures were separated by using the Dionex UltiMate 3000 RSLC nano system (Thermo Fisher Scientific, Waltham, MA, USA). The mobile phase A was composed of 0.1% FA and 5% DMSO in HPLC-grade water (Avantor, Radnor, PA, USA), while the mobile phase B was made up of 0.1% formic acid (FA), 5% DMSO, and 80% HPLC-grade acetonitrile (Avantor) in HPLC-grade water. The dried sample was resuspended in 0.1% formic acid, and their total peptide concentrations were measured using a UV-Vis spectrophotometer (NanoDrop One, Thermo Fisher Scientific) at a wavelength of 280 nm with the sample type option set to "1 Abs = 1 mg/mL.". At a concentration of 1 µg/µL, 5 µL of which was loaded on a C18 Pepmap trap column (20 mm × 100 µm i.d., 5 µm, 100 Å; Thermo Fisher Scientific) and separated with an Acclaim™ Pepmap 100 C18 column (500 mm × 75 µm i.d., 3 µm, 100 Å; Thermo Fisher Scientific) over 200 min (250 nL/min) using a 0–48% acetonitrile gradient in 0.1% formic acid and 5% DMSO for 150 min at 50 °C. The LC was connected with a Q Exactive HF-X mass spectrometer (Thermo Fisher Scientific) with an EASY-Spray nano-ESI source. In a data-dependent mode, mass spectra were obtained with an automatic switch between a full scan

with top 20 data-dependent MS/MS scans. Resolution was set to 60,000 at m/z 200, and target value of 3,000,000 for MS scan type was selected. The ion target value for MS/MS was set at 100,000 with a resolution of 15,000 at m/z 200. The maximum ion injection time was set to 100 ms for the full scan and 50 ms for MS2 scan. Isolation width was 1.7 m/z, and normalized collision energy was set at 27. Dynamic exclusion for measurements of repeated peptides was set for 40 s. All mass spectrometry data were measured once per sample and were deposited in the PRIDE archive (www.ebi.ac.uk/pride/archive/projects/PXD043129; Username: reviewer_pxd043129@ebi.ac.uk, Password: 8A6JzKnl) [16].

2.6 Proteomic identification and quantification

The raw files of tandem mass spectrometry (MS/MS) spectra were matched against the UniProtKB/Swiss-Prot human protein sequence database [17] utilizing SEQUEST HT embedded in Proteome Discoverer (version 2.4; Thermo Fisher Scientific). The search parameters were established at 10 ppm tolerance for precursor ion mass and 0.02 Da for the fragmentation mass. The toleration for trypsin peptides was set at up to two false cleavages, while carbamidomethylation of cysteines was set as a fixed modification, and N-terminal acetylation and methionine oxidation were set as variable modifications. The false discovery rate (FDR) was calculated using the target-decoy search strategy, and the peptides within 1% of the FDR were chosen utilizing the post-processing semi-supervised learning tool Percolator[18] based on the SEQUEST result. In the global proteome analysis, label-free quantification of proteins was performed using the peak intensity for unique and razor peptides of each protein.

2.7 Data analysis

Raw data were analyzed by Perseus software (version 1.6.15.0)[19]. Log2-transformed raw data were normalized by the width adjustment method. For the comparative statistical analysis, protein selection criteria were based on having a quantified value in 70% of at least on group of two groups: IA (N = 9) and control (N = 20). Proteins from sample groups were compared by Student's *t*-test. Results were visualized using RStudio (version 1.3.1093), a component of

R software (version 3.6.0). with the ggplot2 for displaying volcano plots. For all analyses, $P < 0.05$ were considered statistically significant.

2.8 Statistical analysis

The raw data for the average number of technical replicates for each sample were subjected to a log2-transformation and normalized using width adjustment. The different sample groups were compared using ANOVA tests with Benjamini-Hochberg correction, which was performed using the Perseus software (version 1.6.10.50). The results were then visualized using RStudio (version 1.3.1093), which is a component of R software (version 3.6.0). Several other software packages were also utilized, including factoextra for principal component analysis (PCA), PerformanceAnalytics for correlation plotting, ggplot2 for generating boxplots and 2D plots of points, and pheatmap for drawing heatmaps. Statistical significance was defined as a two-tailed test resulting in a p-value less than 0.05, with the inclusion of a false discovery rate (FDR) threshold of less than 0.05.

3. RESULTS

3.1 Patients characteristics

The study compared various parameters between the control group (n=20) and the IA group (n=9) as shown in Table 1. The mean age was similar in both groups, with the control group at 55.90 ± 6.79 years and the IA group at 57.38 ± 5.68 years (p=0.798). The percentage of females was higher in the IA group (66.7%) compared to the control group (45.0%), though this difference was not statistically significant (p=0.280). Both groups had comparable BMI values, with the control group at 23.66 ± 3.30 kg/m² and the IA group at 24.02 ± 3.52 kg/m² (p=0.554). The age at brain imaging study was also similar, with the control group at 55.53 ± 6.60 years and the IA group at 56.66 ± 6.15 years (p=0.959). The proportion of patients who had dialysis before transplantation was nearly the same in both groups, with 75.0% in the control group and 77.8% in the IA group (p=0.872). However, the duration of hemodialysis was significantly longer in the IA group (21.895 ± 37.91 months) compared to the control

group (6.85 ± 11.50 months), with a p-value of 0.001. The presence of PCLD was higher in the IA group (100.0%) than in the control group (75.0%), but this difference was not statistically significant (p=0.099). The history of CVA was similar between the groups, with 30.0% in the control group and 22.2% in the IA group (p=0.665). The prevalence of hypertension was slightly higher in the IA group (88.9%) compared to the control group (80.0%), but this difference was not significant (p=0.558). DM was present in 5.0% of the control group and absent in the IA group (p=0.495). Finally, the estimated Glomerular Filtration Rate (eGFR) was similar in both groups, with the control group at 7.30 ± 2.68 ml/min/1.73m² and the IA group at 6.89 ± 1.53 ml/min/1.73m² (p=0.290). Overall, the significant difference between the two groups was the duration of hemodialysis, which was longer in the IA group.

3.2 Aneurysm characteristics

The study group consisted of 9 patients with IA, comprising of 3 male and 6 female individuals with an average age of 56.6 years (Table 2). The affected arteries were located as follows: 1 left proximal Posterior Inferior Cerebellar Artery (PICA), 2 right Middle Cerebral Artery (MCA) bifurcations, 1 right Internal Carotid Artery (ICA) ophthalmic branch, 2 Superior Cerebellar Arteries (SCA) (1 on the left, 1 on the right), 1 right distal M1 segment, 1 paraclinoid Internal Carotid Arteries (ICAs), and 1 basilar artery top. Each subject had a single intracranial aneurysm, with sizes varying from 1mm to 4mm. This data indicates a diverse distribution of aneurysms across different arterial locations within this cohort.

3.3 Protein identification

Renal artery samples from each group were pooled for proteomic analysis. Upon comparison of the IA and the control group, 8 proteins were identified. Out of these proteins, 4 were upregulated while 4 were downregulated in the group with IA as specified in Table 3. Positive log2 fold-change values denote proteins that are more highly expressed in the IA group, suggesting upregulation. Among the proteins in this category, DIS3 (Exosome complex exonuclease RRP44) exhibits the highest upregulation, with a log2 fold-change of 2. RAB6A (Isoform 2 of Ras-related protein Rab-6A) follows closely with a log2 fold-change of 1.97.

Other proteins with positive fold-change include MMS19 (MMS19 nucleotide excision repair protein homolog) and EXOC8 (Exocyst complex component 8), with log2 fold-changes of 1.13 and 1.09, respectively.

Conversely, negative log2 fold-change values indicate proteins that are more highly expressed in the control group, suggesting downregulation in the IA group. CLUH (Clusted mitochondria protein homolog), SYCN (Syncollin) and MEF2D (Myocyte-specific enhancer factor 2D) display significant downregulation with log2 fold-changes of -1.84, -2.61 and -2.93, respectively. The most substantial downregulation is observed in WDR36 (WD repeat-containing protein 36), with a log2 fold-change of -3.97.

The FDR q-value serves as an indicator of statistical significance. SYCN and WDR36, with FDR q-values of 0, demonstrate the highest confidence in differential expression. Other proteins with significant FDR q-values include DIS3 (0.0451), RAB6A (0.048), MMS19 (0.0107), EXOC8 (0.044), and CLUH (0.0447).

3.4 Correlation between candidate protein expressions and laboratory variables

Table 4 presents the correlation between candidate protein expressions and laboratory variables in the study group, highlighting significant relationships. The protein MMS19 shows a negative correlation with platelet count ($r = -0.59$, $p < 0.0001$) and positive correlations with total bilirubin ($r = 0.397$, $p = 0.032$), PT (sec) ($r = 0.391$, $p = 0.047$), and PT (INR) ($r = 0.447$, $p = 0.021$). The protein SYCN is positively correlated with platelet count ($r = 0.558$, $p < 0.001$) and negatively correlated with PT (sec) ($r = -0.497$, $p = 0.003$). MEF2D shows a positive correlation with platelet count ($r = 0.432$, $p = 0.02$). Finally, WDR36 is positively correlated with platelet count ($r = 0.557$, $p = 0.001$) and negatively correlated with total bilirubin ($r = -0.368$, $p = 0.049$). These correlations suggest significant associations between these proteins and specific laboratory variables in the study group.

4. DISCUSSION

Intracranial aneurysms in ADPKD patients present a significant clinical challenge due to the increased risk of rupture, leading to subarachnoid hemorrhage, a condition with high morbidity and mortality rates. The connection between ADPKD and the development of

intracranial aneurysms is believed to be related to abnormalities in the blood vessels and the cystic nature of the disease, which may predispose individuals to weakened arterial walls[20,21]. Molecular studies provide insight into how ADPKD contributes to vascular abnormalities. Research has shown that polycystin 1, a protein encoded by the PKD1 gene, is crucial for the structural integrity of blood vessels. Mutations in the PKD1 and PKD2 genes, which are common in ADPKD, result in altered calcium signaling in vascular smooth muscle cells, impacting vascular reactivity and potentially leading to the development of intracranial aneurysms[21].

Currently, the detection and monitoring of intracranial aneurysms in PCKD patients rely heavily on imaging techniques such as MRA and CTA. While these methods are effective in identifying the presence of aneurysms, they do not provide insights into the risk of aneurysm growth or rupture until potentially life-threatening symptoms emerge. This limitation underscores a critical need for novel biomarkers that can offer prognostic value, enabling early intervention and personalized management strategies for at-risk patients.

Despite extensive research, the search for reliable biomarkers for intracranial aneurysms, particularly in the context of ADPKD, has been challenging. Factors such as the heterogeneity of the disease, the complexity of aneurysm biology, and the interplay between genetic and environmental factors contribute to the difficulty in identifying specific proteins or molecular signatures that could serve as early indicators of aneurysm formation or risk of rupture.

In this context, our research represents a groundbreaking effort to identify novel proteins through comprehensive proteomic analysis. By employing advanced techniques such as mass spectrometry and bioinformatics, we have uncovered a set of proteins not previously discovered to be associated with intracranial aneurysms in ADPKD patients. These proteins offer promising potential as biomarkers for early diagnosis, risk assessment, and monitoring aneurysm progression.

Possible novel candidate proteins

EXOC8

EXOC8 is one of the subunits in the exocyst complex which is made up of eight subunit, EXOC1–EXOC8. The complex has been recognized for its involvement in diverse cellular activities including exocytosis, cell growth and migration, cell polarity, cytokinesis, ciliogenesis and autophagy[22-25]. Previous research has indicated that mutations in EXOC8 play a crucial role in a neurodevelopmental disorder marked by microcephaly, seizures, and brain atrophy, which is associated with Joubert syndrome[26,27]. Joubert syndrome itself features a unique pattern of cerebellum and midbrain abnormalities, often accompanied by symptoms common to polycystic kidney disease[28]. Classified among ciliopathies, these disorders stem from defects in cilia's structure and function. Notably, a significant number of Joubert syndrome patients may also develop polycystic kidney disease as a part of their condition. As a ciliary proteome component, EXOC8's mutation is believed to contribute to Joubert syndrome by disrupting ciliary function, highlighting its importance among the many genes linked to this ciliopathy[29].

Recent studies underscore the critical role of primary cilia in vascular integrity, noting that their deficiency may lead to aneurysm formation[30]. Additionally, research on animals has shown a significant reduction in the number of cells with primary cilia in the aneurysm-prone regions of mice. The disruption of genes like Polycystin 1, Polycystin 2, and Intraflagellar Transport 88 heightened the mice's susceptibility to developing IAs. This evidence, coupled with the observation of increased mutation frequencies in IA patients' genes related to primary cilia, suggests that the link between primary cilia deficiency and IA development is consistent across species[31]. In summary, the involvement of EXOC8 in the formation of intracranial aneurysms in ADPKD patients can be attributed to its critical role in the exocyst complex and ciliogenesis.

RAB6A

RAB6A, a small GTP/GDP-binding protein, facilitates protein transport from the endoplasmic reticulum to the Golgi apparatus and plasma membrane[32]. It plays a crucial role in macrophages' secretion of pro-inflammatory cytokines, notably TNF-alpha[33], which is significantly involved in the inflammatory processes weakening arterial walls and thus

contributing to the development and rupture of cerebral aneurysms[34]. Shi et al. utilized microarray techniques to analyze gene expression in human IA lesions, uncovering an association between inflammation, inflammatory response, apoptosis, and IA development. They also noted an upregulation of proinflammatory genes, including TNF-α, in the walls of human IAs[35]. This connection between Rab6a and TNF-alpha underscores its critical role in the pathophysiology of intracranial aneurysms.

Moreover, RAB6A's role in the phenotypic modulation of smooth muscle cells under hypoxic conditions further underscores its significant impact on vascular health and aneurysm development[36]. This suggests RAB6A's involvement extends beyond immune function, influencing vascular remodeling and health. This aspect of RAB6a's function may have indirect but profound implications in the context of cerebral aneurysm formation, suggesting a multi-faceted role in vascular pathology.

Our findings suggest that targeting the RAB6a and TNF-alpha pathways could offer new therapeutic avenues for managing the inflammation and arterial weakening that lead to aneurysms. Understanding RAB6a's mechanism in regulating TNF-alpha secretion could unveil novel targets for therapy, offering hope for better treatments for cerebral aneurysm patients. This emphasizes the potential of focusing on the RAB6a and TNF-alpha pathways as therapeutic strategies in preventing and managing intracranial aneurysms.

MMS19

MMS19 acts as a coactivator for estrogen receptor (ER) transcription by facilitating the incorporation of iron-sulfur into specific components of the TFIIH complex. MMS19 interacts with nuclear receptors and bind with ERα[37]. Estrogen has been found to have vasoprotective effects, including anti-inflammatory properties and the ability to promote smooth muscle cell proliferation and collagen synthesis, which strengthen the arterial wall[38,39]. And this fact was clinically shown by multiple studies that show a correlation between hormon replacement therapy containing estrogen and a decreased incidence of intracranial aneurysmysmal hemmorrhages. Therefore, the activation of estrogen receptors might play a role in these

vasoprotective effects. Thus, as a coactivator, MMS19 enhances the transcriptional activity of ER by interacting with it and assisting in the recruitment of the transcriptional machinery to estrogen-responsive genes, resulting in amplifying the vasoprotective effects of estrogen[40-42].

Interestingly, our proteomic analysis revealed that MMS19 is upregulated in the intracranial aneurysm group compared to the control group. MMS19 is known for its vasoprotective effects via activation of estrogen receptors, which initially seems paradoxical. However, we hypothesize that this upregulation may be a compensatory response to increased vascular stress and damage. The body might be attempting to utilize MMS19's protective properties to counteract the pathological processes leading to aneurysm formation. Despite this upregulation, the complex interplay of other pro-inflammatory and pro-aneurysmal factors might be overwhelming its protective effects. This finding underscores the importance of understanding the dynamic and context-dependent nature of protein regulation and highlights the need for further research into these mechanisms.

WDR36

WDR36 is associated with various cellular processes, including cell cycle progression, signal transduction, apoptosis, and gene regulation. Disruption of WDR36 in human trabecular meshwork cells leads to apoptosis and an increase in the expressions of P53, P21, and BAX[43]. In a study by Kondo et al., the role of apoptosis in medial smooth muscle cells (SMCs) in the development of saccular cerebral aneurysms in rats was investigated. Techniques like in situ end labeling of fragmented DNA and electron microscopy were used to explore the connection between SMC apoptosis and aneurysm formation. The study revealed a correlation between medial SMC apoptosis and the formation of saccular cerebral aneurysms in rats[44].

Additionally, WDR36 is implicated in Jeune syndrome, or asphyxiating thoracic dystrophy, due to its potential effects on ciliary function and ribosome biogenesis[45]. Jeune syndrome is characterized by skeletal abnormalities, such as a narrow, bell-shaped chest and shortened

ribs, primarily caused by mutations in genes involved in the intraflagellar transport (IFT) system essential for cilia function. Although WDR36 is not a primary gene associated with Jeune syndrome, it is crucial for ribosome biogenesis, which is essential for protein synthesis, including proteins necessary for cilia structure and function.

Association of polycystic liver disease with IA occurrences

PCLD frequently occurs alongside PCKD in ADPKD patients, leading to a clinical situation characterized by a marked increase in liver cyst growth. When PCLD and PCKD coexist, patients often see an escalation in both the number and size of liver cysts over time, potentially impacting liver functionality[46]**.** Despite these developments, the liver enzyme levels and function tests for most individuals with PCLD typically remain within or near normal ranges. Nonetheless, individuals displaying symptoms often present with laboratory abnormalities, including increased levels of alkaline phosphatase, gamma-glutamyl transpeptidase, aspartate aminotransferase, and total bilirubin, with prevalence rates ranging from 15% to 70% [47]. Our analysis revealed that certain candidate proteins, such as MMS19, SYCN, MEF2D, and WDR36, exhibited correlations with laboratory test abnormalities, including platelet counts, total bilirubin levels, and PT as listed in Table 4.

With age, ADPKD patients tend to exhibit more frequent symptoms and complications, highlighting a progression in the severity of the disease that corresponds with an escalation in disease-related symptoms[48]. A longitudinal study by R. Matsuura et al. on ADPKD patients, comparing those with and without concurrent PCLD, indicated similar platelet counts across both groups, albeit slightly lower in PCLD patients. This study also noted a steady increase in liver cyst size over time, with no reduction, and found no significant link between the volume of liver cysts and the overall liver volume [49]. This discrepancy implies that cyst growth could lead to a reduction in liver parenchyma volume, potentially affecting coagulation functions as suggested by aggravation of platelet counts and prothrombin time.

Moreover, certain studies have highlighted that an increase in liver volume in PCLD patients could lead to deteriorating liver function, eventually requiring a liver transplant as

the only viable treatment option[50,51]. Observational research has further established a significant association between the progression of renal cysts or renal dysfunction and the development of liver cysts [52-54]. In the autopsy series conducted by Karhunen and Tenhu, it was found that six out of twelve cases of ADPKD, regardless of the presence of PCLD, had IAs. Conversely, none of the ten cases with isolated polycystic liver disease exhibited intracranial aneurysms. This finding indicates that the coexistence of polycystic liver disease with ADPKD may elevate the risk of developing IAs. If a correlation exists between liver enzyme levels, affected by the volume impact of PCLD, and the incidence of IAs, assessing liver enzyme levels could serve as an indirect method to gauge the risk of IAs[55].

Limitations

There are some potential limitations of our study on the proteomic analysis for diagnosing IAs in ADPKD patients. The retrospective design of our study may limit the ability to establish causality between the identified protein biomarkers and the development of IAs in ADPKD patients. Retrospective analyses often rely on the availability and accuracy of existing data, which can introduce biases and affect the generalizability of the findings. The utilization of renal artery samples, rather than directly analyzing tissue from intracranial aneurysms, may not fully capture the specific proteomic changes occurring in the aneurysmal sites. While renal arteries in ADPKD patients are relevant due to the systemic nature of the disease, the proteomic profile of IAs might differ significantly due to the unique pathophysiological conditions in the cerebral vasculature. This discrepancy could influence the applicability of the identified biomarkers for diagnosing IAs specifically. In addition, a larger and more diverse sample size would enhance the reliability of the biomarkers discovered in the present study. While the study validated the increased expression of the candidate proteins through immunoblotting, further validation in independent cohorts is necessary to confirm these findings. Independent validation would help to establish the consistency of these biomarkers across different populations and settings. Given the complexity of ADPKD and the development of IAs, there may be confounding factors that were not fully accounted for in the study. These could include variations in treatment regimens, comorbid conditions, and

lifestyle factors that might influence the proteomic profile of patients. Addressing these limitations in future research will be essential for confirming the potential diagnostic value of the candidate proteins for IAs in ADPKD patients. Further studies should aim to include prospective designs, direct analysis of aneurysmal tissue, larger and more diverse sample sizes, and comprehensive strategies to mitigate confounding factors.

5. Conclusion

In this study, we have unveiled a set of biomarkers through advanced proteomic analyses, that not only enhance our understanding of the pathophysiological mechanisms underpinning aneurysm development in ADPKD but also hold promise for revolutionizing the early detection and management of this critical condition. The implications of our findings extend beyond the immediate sphere of ADPKD-associated IAs, offering a new perspective on the potential for proteomic technologies to uncover biomarkers for other cerebrovascular conditions. While further validation and clinical trials are necessary to translate these biomarkers into practical diagnostic tools, our research paves the way for the development of non-invasive, accurate, and early diagnostic methods that could significantly improve patient outcomes through timely intervention.

As we move forward, it is crucial for ongoing and future studies to build upon our findings, exploring the full diagnostic and therapeutic potential of these and other novel proteins. Collaborative, interdisciplinary research efforts will be key to translating these biomarkers from the laboratory to the clinic, ultimately enhancing the precision and effectiveness of care for patients with ADPKD at risk of developing intracranial aneurysms. Our study marks an important step in this journey, highlighting the role of innovative proteomic technologies in advancing our understanding of complex diseases and bringing us closer to personalized medicine.

6. References

1. Niemczyk M, Niemczyk S, Paczek L. Autosomal dominant polycystic kidney disease and transplantation. *Ann Transplant*. Oct-Dec 2009;14(4):86-90.
2. Suwabe T, Shukoor S, Chamberlain AM, et al. Epidemiology of Autosomal Dominant Polycystic Kidney Disease in Olmsted County. *Clin J Am Soc Nephrol*. Jan 7 2020;15(1):69-79. doi:10.2215/cjn.05900519
3. Kim JY, Jung SC, Ko Y, et al. Intracranial aneurysms in patients receiving kidney transplantation for autosomal dominant polycystic kidney disease. *Acta Neurochir (Wien)*. Nov 2019;161(11):2389-2396. doi:10.1007/s00701-019-04060-7
4. Chauveau D, Pirson Y, Verellen-Dumoulin C, Macnicol A, Gonzalo A, Grünfeld JP. Intracranial aneurysms in autosomal dominant polycystic kidney disease. *Kidney Int*. Apr 1994;45(4):1140-6. doi:10.1038/ki.1994.151
5. Gabow PA. Autosomal dominant polycystic kidney disease. *N Engl J Med*. Jul 29 1993;329(5):332-42. doi:10.1056/nejm199307293290508
6. Huston J, 3rd, Torres VE, Sulivan PP, Offord KP, Wiebers DO. Value of magnetic resonance angiography for the detection of intracranial aneurysms in autosomal dominant polycystic kidney disease. *J Am Soc Nephrol*. Jun 1993;3(12):1871-7. doi:10.1681/asn.V3121871
7. Sanchis IM, Shukoor S, Irazabal MV, et al. Presymptomatic Screening for Intracranial Aneurysms in Patients with Autosomal Dominant Polycystic Kidney Disease. *Clin J Am Soc Nephrol*. Aug 7 2019;14(8):1151-1160. doi:10.2215/cjn.14691218
8. Gibbs GF, Huston J, 3rd, Qian Q, et al. Follow-up of intracranial aneurysms in autosomal-dominant polycystic kidney disease. *Kidney Int*. May 2004;65(5):1621-7. doi:10.1111/j.1523-1755.2004.00572.x
9. Irazabal MV, Huston J, 3rd, Kubly V, et al. Extended follow-up of unruptured intracranial aneurysms detected by presymptomatic screening in patients with autosomal dominant polycystic kidney disease. *Clin J Am Soc Nephrol*. Jun 2011;6(6):1274-85. doi:10.2215/cjn.09731110
10. Ekinci İ, Buyukkaba M, Cinar A, et al. Endothelial Dysfunction and Atherosclerosis in Patients With Autosomal Dominant Polycystic Kidney Disease. *Cureus*. Feb 25 2021;13(2):e13561. doi:10.7759/cureus.13561
11. Horie S, Mochizuki T, Muto S, et al. Evidence-based clinical practice guidelines for polycystic kidney disease 2014. *Clin Exp Nephrol*. Aug 2016;20(4):493-509. doi:10.1007/s10157-015-1219-7
12. Yoshida H, Higashihara E, Maruyama K, et al. Relationship between intracranial aneurysms and the severity of autosomal dominant polycystic kidney disease. *Acta Neurochir (Wien)*. Dec 2017;159(12):2325-2330. doi:10.1007/s00701-017-3316-8
13. Rangan GK, Lee VW, Alexander SI, Patel C, Tunnicliffe DJ, Vladica P. KHA-CARI Autosomal Dominant Polycystic Kidney Disease Guideline: Screening for Polycystic Kidney Disease. *Semin Nephrol*. Nov 2015;35(6):557-564.e6. doi:10.1016/j.semnephrol.2015.10.004
14. Harris PC, Torres VE. Polycystic Kidney Disease, Autosomal Dominant. In: Adam MP, Feldman J, Mirzaa GM, et al, eds. *GeneReviews(®)*. University of Washington, Seattle

15. Pei Y, Hwang YH, Conklin J, et al. Imaging-based diagnosis of autosomal dominant polycystic kidney disease. *J Am Soc Nephrol*. Mar 2015;26(3):746-53. doi:10.1681/asn.2014030297
16. Perez-Riverol Y, Csordas A, Bai J, et al. The PRIDE database and related tools and resources in 2019: improving support for quantification data. *Nucleic Acids Res*. Jan 8 2019;47(D1):D442-d450. doi:10.1093/nar/gky1106
17. UniProt: the Universal Protein Knowledgebase in 2023. *Nucleic Acids Res*. Jan 6 2023;51(D1):D523-d531. doi:10.1093/nar/gkac1052
18. Käll L, Canterbury JD, Weston J, Noble WS, MacCoss MJ. Semi-supervised learning for peptide identification from shotgun proteomics datasets. *Nat Methods*. Nov 2007;4(11):923-5.

doi:10.1038/nmeth1113
19. Tyanova S, Cox J. Perseus: A Bioinformatics Platform for Integrative Analysis of Proteomics Data in Cancer Research. *Methods Mol Biol*. 2018;1711:133-148. doi:10.1007/978-1-4939-7493-1_7
20. Fehlings MG, Gentili F. The association between polycystic kidney disease and cerebral aneurysms. *Can J Neurol Sci*. Nov 1991;18(4):505-9. doi:10.1017/s0317167100032248
21. Perrone RD, Malek AM, Watnick T. Vascular complications in autosomal dominant polycystic kidney disease. *Nat Rev Nephrol*. Oct 2015;11(10):589-98. doi:10.1038/nrneph.2015.128
22. Heider MR, Munson M. Exorcising the exocyst complex. *Traffic*. Jul 2012;13(7):898-907. doi:10.1111/j.1600-0854.2012.01353.x
23. Luo G, Zhang J, Luca FC, Guo W. Mitotic phosphorylation of Exo84 disrupts exocyst assembly and arrests cell growth. *J Cell Biol*. Jul 8 2013;202(1):97-111. doi:10.1083/jcb.201211093
24. Wu B, Guo W. The Exocyst at a Glance. *J Cell Sci*. Aug 15 2015;128(16):2957-64. doi:10.1242/jcs.156398
25. He B, Guo W. The exocyst complex in polarized exocytosis. *Curr Opin Cell Biol*. Aug 2009;21(4):537-42. doi:10.1016/j.ceb.2009.04.007
26. Dixon-Salazar TJ, Silhavy JL, Udpa N, et al. Exome sequencing can improve diagnosis and alter patient management. *Sci Transl Med*. Jun 13 2012;4(138):138ra78. doi:10.1126/scitranslmed.3003544
27. Coulter ME, Musaev D, DeGennaro EM, et al. Regulation of human cerebral cortical development by EXOC7 and EXOC8, components of the exocyst complex, and roles in neural progenitor cell proliferation and survival. *Genet Med*. Jun 2020;22(6):1040-1050. doi:10.1038/s41436-020-0758-9
28. Joubert M, Eisenring JJ, Robb JP, Andermann F. Familial agenesis of the cerebellar vermis. A syndrome of episodic hyperpnea, abnormal eye movements, ataxia, and retardation. *Neurology*. Sep 1969;19(9):813-25. doi:10.1212/wnl.19.9.813
29. Halim DO, Munson M, Gao FB. The exocyst complex in neurological disorders. *Hum Genet*. Aug 2023;142(8):1263-1270. doi:10.1007/s00439-023-02558-w
30. Van der Heiden K, Egorova AD, Poelmann RE, Wentzel JJ, Hierck BP. Role for primary cilia as flow detectors in the cardiovascular system. *Int Rev Cell Mol Biol*. 2011;290:87-119. doi:10.1016/b978-0-12-386037-8.00004-1
31. Liu M, Zhao J, Zhou Q, Peng Y, Zhou Y, Jiang Y. Primary Cilia Deficiency Induces Intracranial Aneurysm. *Shock*. May 2018;49(5):604-611. doi:10.1097/shk.0000000000000961
32. Bergbrede T, Chuky N, Schoebel S, et al. Biophysical analysis of the interaction of Rab6a GTPase with its effector domains. *J Biol Chem*. Jan 30 2009;284(5):2628-2635. doi:10.1074/jbc.M806003200
33. Micaroni M, Stanley AC, Khromykh T, et al. Rab6a/a' are important Golgi regulators of pro-inflammatory TNF secretion in macrophages. *PLoS One*. 2013;8(2):e57034. doi:10.1371/journal.pone.0057034
34. Jayaraman T, Paget A, Shin YS, et al. TNF-alpha-mediated inflammation in cerebral aneurysms: a potential link to growth and rupture. *Vasc Health Risk Manag*. 2008;4(4):805-17. doi:10.2147/vhrm.s2700
35. Shi C, Awad IA, Jafari N, et al. Genomics of human intracranial aneurysm wall. *Stroke*. Apr 2009;40(4):1252-61. doi:10.1161/strokeaha.108.532036
36. Wang F, Xu X, Tang W, Min L, Yang J. Rab6A GTPase contributes to phenotypic modulation in pulmonary artery smooth muscle cells under hypoxia. *J Cell Biochem*. May 2019;120(5):7858-7867. doi:10.1002/jcb.28060
37. Wu X, Li H, Chen JD. The human homologue of the yeast DNA repair and TFIIH regulator MMS19 is an AF-1-specific coactivator of estrogen receptor. *J Biol Chem*. Jun 29 2001;276(26):23962-8. doi:10.1074/jbc.M101041200
38. Song J, Wan Y, Rolfe BE, Campbell JH, Campbell GR. Effect of estrogen on vascular smooth muscle cells is dependent upon cellular phenotype. *Atherosclerosis*. Sep 1998;140(1):97-104. doi:10.1016/s0021-9150(98)00122-1

39. Khastgir G, Studd J, Holland N, Alaghband-Zadeh J, Sims TJ, Bailey AJ. Anabolic effect of long-term estrogen replacement on bone collagen in elderly postmenopausal women with osteoporosis. *Osteoporos Int*. 2001;12(6):465-70. doi:10.1007/s001980170091
40. Longstreth WT, Nelson LM, Koepsell TD, van Belle G. Subarachnoid hemorrhage and hormonal factors in women. A population-based case-control study. *Ann Intern Med*. Aug 1 1994;121(3):168-73. doi:10.7326/0003-4819-121-3-199408010-00002
41. Mhurchu CN, Anderson C, Jamrozik K, Hankey G, Dunbabin D. Hormonal factors and risk of aneurysmal subarachnoid hemorrhage: an international population-based, case-control study. *Stroke*. Mar 2001;32(3):606-12. doi:10.1161/01.str.32.3.606
42. Iorga A, Cunningham CM, Moazeni S, Ruffenach G, Umar S, Eghbali M. The protective role of estrogen and estrogen receptors in cardiovascular disease and the controversial use of estrogen therapy. *Biol Sex Differ*. Oct 24 2017;8(1):33. doi:10.1186/s13293-017-0152-8
43. Gallenberger M, Meinel DM, Kroeber M, et al. Lack of WDR36 leads to preimplantation embryonic lethality in mice and delays the formation of small subunit ribosomal RNA in human cells in vitro. *Hum Mol Genet*. Feb 1 2011;20(3):422-35. doi:10.1093/hmg/ddq478
44. Kondo S, Hashimoto N, Kikuchi H, Hazama F, Nagata I, Kataoka H. Apoptosis of medial smooth muscle cells in the development of saccular cerebral aneurysms in rats. *Stroke*. Jan 1998;29(1):181-8; discussion 189. doi:10.1161/01.str.29.1.181
45. Kim Y, Kim SH. WD40-Repeat Proteins in Ciliopathies and Congenital Disorders of Endocrine System. *Endocrinol Metab (Seoul)*. Sep 2020;35(3):494-506. doi:10.3803/EnM.2020.302
46. Morgan DE, Lockhart ME, Canon CL, Holcombe MP, Bynon JS. Polycystic liver disease: multimodality imaging for complications and transplant evaluation. *Radiographics*. Nov-Dec 2006;26(6):1655-68; quiz 1655. doi:10.1148/rg.266065013
47. Arnold HL, Harrison SA. New advances in evaluation and management of patients with polycystic liver disease. *Am J Gastroenterol*. Nov 2005;100(11):2569-82. doi:10.1111/j.1572-0241.2005.00263.x
48. Lantinga MA, Drenth JP, Gevers TJ. Diagnostic criteria in renal and hepatic cyst infection. *Nephrol Dial Transplant*. May 2015;30(5):744-51. doi:10.1093/ndt/gfu227
49. Matsuura R, Honda K, Hamasaki Y, Doi K, Noiri E, Nangaku M. The Longitudinal Study of Liver Cysts in Patients With Autosomal Dominant Polycystic Kidney Disease and Polycystic Liver Disease. *Kidney Int Rep*. Jan 2017;2(1):60-65. doi:10.1016/j.ekir.2016.09.061
50. Gringeri E, D'Amico FE, Bassi D, et al. Liver transplantation for massive hepatomegaly due to polycystic liver disease: an extreme case. *Transplant Proc*. Sep 2012;44(7):2038-40. doi:10.1016/j.transproceed.2012.06.041
51. Fonseca Neto O, Martins BCN, Jucá NT, et al. Combined liver-kidney transplant in polycystic diseases: a case report. *Einstein (Sao Paulo)*. 2023;21:eRC0282. doi:10.31744/einstein_journal/2023RC0282
52. Gabow PA, Johnson AM, Kaehny WD, Manco-Johnson ML, Duley IT, Everson GT. Risk factors for the development of hepatic cysts in autosomal dominant polycystic kidney disease. *Hepatology*. Jun 1990;11(6):1033-7. doi:10.1002/hep.1840110619
53. Grünfeld JP, Albouze G, Jungers P, et al. Liver changes and complications in adult polycystic kidney disease. *Adv Nephrol Necker Hosp*. 1985;14:1-20.
54. Bae KT, Zhu F, Chapman AB, et al. Magnetic resonance imaging evaluation of hepatic cysts in early autosomal-dominant polycystic kidney disease: the Consortium for Radiologic Imaging Studies of Polycystic Kidney Disease cohort. *Clin J Am Soc Nephrol*. Jan 2006;1(1):64-9. doi:10.2215/cjn.00080605
55. Karhunen PJ, Tenhu M. Adult polycystic liver and kidney diseases are separate entities. *Clin Genet*. Jul 1986;30(1):29-37. doi:10.1111/j.1399-0004.1986.tb00565.x

국문요약

두개강내 동맥류(intracranial aneurysm, IA)는 상염색체우성 다낭신 (autosomal dominant polycystic kidney disease, ADPKD)과 자주 동반되며, 일반 인구에 비해 약 10 배 높은 발병률을 보인다. 그러나 이 두 가지 상태가 어떻게 관련되어 있는지에 대한 정확한 메커니즘은 아직 불분명하다. 이 연구는 단백질체학을 이용하여 ADPKD 환자에서 IA 발생 메커니즘을 확인하고 조기 진단을 위한 잠재적인 단백질 바이오마커를 발견하는 것을 목표로 한다.

신장 이식 전 ADPKD 환자들은 두개 CT 및/또는 MR 혈관조영술을 받았으며, 그 결과에 따라 대조군(IA 없는 ADPKD, n=20) 또는 IA 군(IA 동반 ADPKD, n=9)으로 배정되었다. 이식 중에는 양측 신장적출술이 시행되었고 고유 신동맥 표본을 채취하여 액체 크로마토그래피-탄뎀 질량분석기를 통한 단백질체 분석을 실시했다. 발현량이 차이 나는 단백질들은 생물정보학 분석과 단백질-단백질 상호작용 네트워크 분석을 거쳤다.

IA 군과 대조군 사이에서 8 개의 단백질이 유의미한 변화를 보였는데, 4 개 단백질(DIS3, MMS19, EXOC8, RAB6A)은 상향 조절되었고 4 개 단백질(CLUH, SYNC, MEF2D, WDR36)은 대조군에 비해 IA 군에서 하향 조절되었다(Log2 폴드 변화(FC) >2 및 가짜발견율(FDR) q-값 <0.05). 이러한 단백질들은 섬유질병증, 배출, 염증, 세포외 기질 재형성, 세포자멸사 등 IA 발달과 관련된 경로들과 연관되어 있었다. 이 단백질들은 면역블로팅을 통해 정량적으로 검증되었으며, 단백질체 데이터와 일치하는 것으로 나타났다. 더불어 단백질 발현량과 임상 지표(빌리루빈, 프로트롬빈 시간, 혈소판 수치) 사이에 연관성이 관찰되어 조기 진단 마커로서의 가능성을 시사했다.

본 연구는 ADPKD 환자에서 IA 의 근본 메커니즘을 단백질체학을 통해 연구하기 위해 신동맥 표본을 사용한 최초의 연구다. 우리는 IA 군에서 대조군에 비해 상향 또는 하향 조절된 새로운 후보 마커들을 발견하고 검증했다. 본 연구 결과는 ADPKD 에서 IA 를 이해하고 진단하는 새로운 방향을 제시하며, 앞으로 조기 진단과 표적 치료로 이어질 수 있을 것이다.

Table 1. Comparison of demographic and clinical characteristics between control and IA groups

Variable	Control (n=20)	IA (n=9)	P-value
Age (years; mean±SD)	55.90 ± 6.79	57.38 ± 5.68	0.798
Female (n[%])	9(45.0%)	6(66.7%)	0.280
BMI (kg/m2; mean±SD)	23.66 ± 3.30	24.02 ± 3.52	0.554
Age at brain imaging study (years; mean±SD)	55.53 ± 6.60	56.66 ± 6.15	0.959
Any dialysis before transplantation (n[%])	15(75.0%)	7(77.8%)	0.872
HD duration (month; mean±SD)	6.85 ± 11.50	21.895 ± 37.91	0.001
PCLD (n[%])	15(75.0%)	9(100.0%)	0.099
CVA Hx (n[%])	0 (0.0%)	2(22.2%)	0.665
HTN (n[%])	16(80.0%)	8(88.9%)	0.558
DM (n[%])	1(5.0%)	0(0.0%)	0.495
eGFR (ml/min/1.73m2; mean±SD)	7.30 ± 2.68	6.89± 1.53	0.290

*BMI: body mass index, PCLD: polycystic liver disease, CVA: cerobrovascular accident, HTN: hypertension, DM: diabetes mellitus, eGFR: estimated glomerular filtration rate

Table 2. Aneurysm details in intracranial aneurysm group

Subject No.	Age/Sex	Intracranial aneurysms		
		Number	Size(mm)	Arteries affected
1	60/F	1	2.5	Left proximal PICA
2	61/F	1	2.7	Right MCA bifurcation
3	48/M	1	2	Right ICA opthalmic
4	53/F	1	4	Right SCA
5	59/F	1	2	Left SCA
6	50/F	1	3	Right distal M1
7	66/M	1	3	Right MCA bifurcation
8	59/F	1	1	Paraclinoid ICA
9	53/M	1	1	Basilar artery

* PICA, posterior inferior cerebellar artery; MCA, middle cerebral artery; ICA, internal carotid artery; SCA, superior cerebellar artery

Table 3. Comparative analysis of gene expression and protein levels in control vs. intracranial aneurysm group

Control vs. IA group

Gene	Protein	FDR q-value	Log2 fold-change (A/C)
DIS3	Exosome complex exonuclease RRP44	0.0451	2
RAB6A	Isoform 2 of Ras-related protein Rab-6A	0.048	1.97
MMS19	MMS19 nucleotide excision repair protein homolog	0.0107	1.13
EXOC8	Exocyst complex component 8	0.044	1.09
CLUH	Clustered mitochondria protein homolog	0.0447	-1.84
SYCN	Syncollin	0	-2.61
MEF2D	Myocyte-specific enhancer factor 2D	0.011	-2.93
WDR36	WD repeat-containing protein 36	0	-3.97

Table 4. Correlation between candiate protein expressions and laboratory variables in the study group.

Protein	Laboratory variables	Pearson Correlation Coefficients	P-value
MMS19	Platelet	-0.59	<0.0001
MMS19	Total bilirubin	0.397	0.032
MMS19	PT(sec)	0.391	0.047
MMS19	PT(INR	0.447	0.021
SYCN	Platelet	0.558	<0.001
SYCN	PT(sec)	-0.497	0.003
MEF2D	Platelet	0.432	0.02
WDR36	Platelet	0.557	0.001
WDR36	Total bilirubin	-0.368	0.049

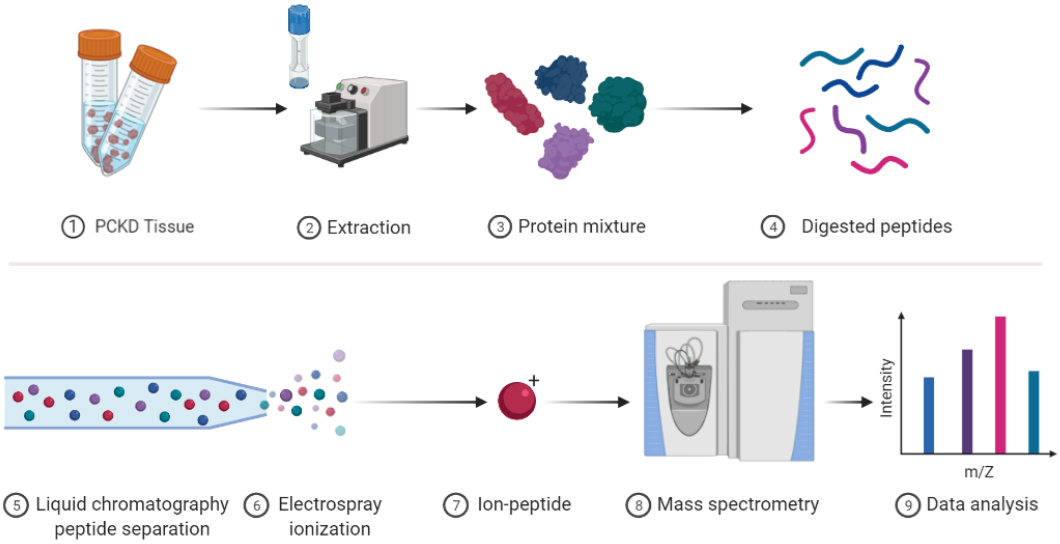

Figure 1. Proteomic analysis workflow of PKCD tissue samples. This schematic diagram outlines the comprehensive steps undertaken in the proteomic analysis of polycystic kidney disease (PKCD) tissue samples. (A) Sample preparation is initiated with the collection of PKCD tissue (1), followed by protein extraction via mechanical homogenization (2), resulting in a complex protein mixture (3). Subsequent enzymatic digestion breaks down proteins into peptides (4). (B) The analytical phase commences with the separation of peptides using liquid chromatography (5), which are then ionized by electrospray (6). The ionized peptides (7) are introduced into a mass spectrometer (8) that measures their mass-to-charge (m/z) ratios. The resulting data are analyzed to yield a bar graph (9), representing the relative intensities of the detected ions, which facilitates the identification and quantification of peptides present in the sample. Each step is depicted with representative icons and images to illustrate the transition from tissue samples to analyzable molecular data.

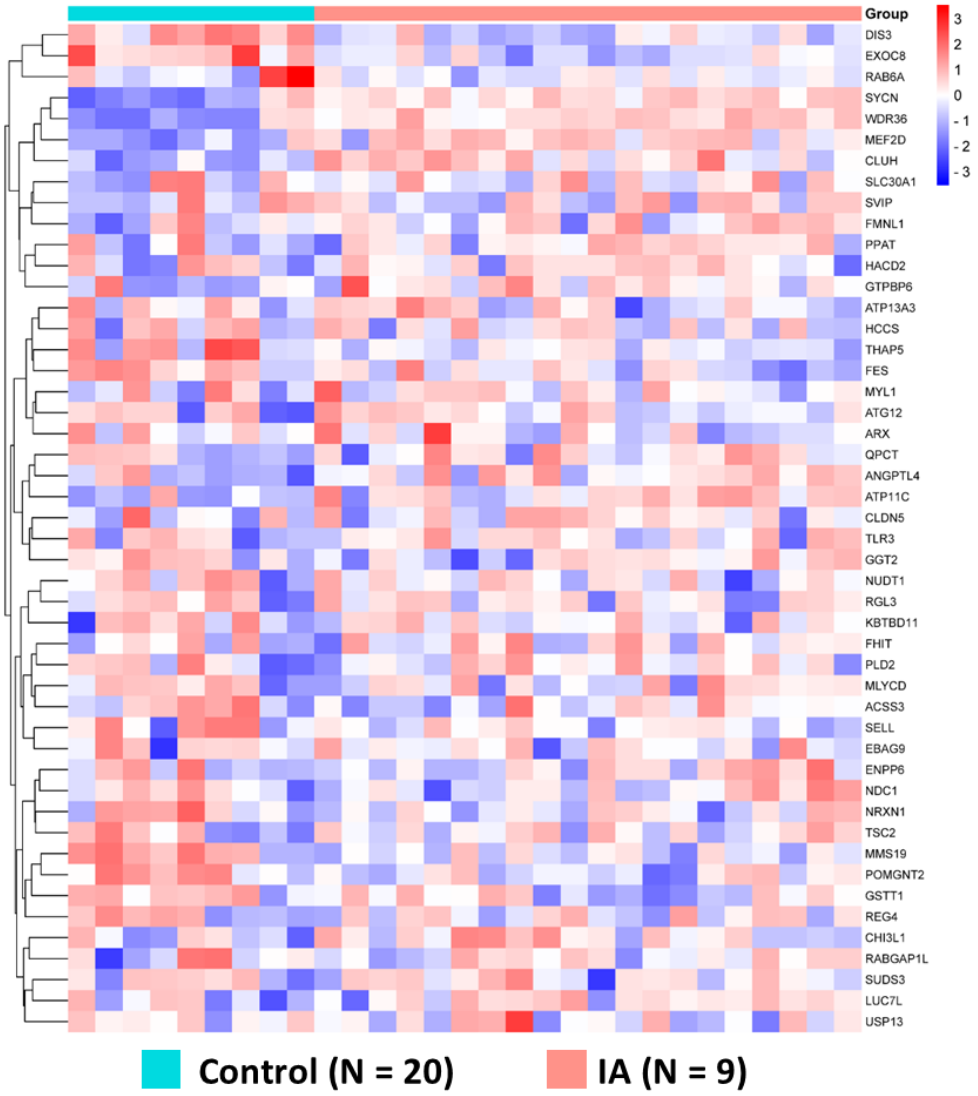

Figure 2. Heatmap visualization of proteomic expression in control and aneurysm groups. The heatmap presents the protein expression profiles across three different groups: control (N = 20), and aneurysm (N = 9). Each row signifies an individual protein, and each column corresponds to a sample within the study groups. The color gradient reflects protein expression levels, with red for upregulation and blue for downregulation. The hierarchical clustering of the samples, based on their similarity or dissimilarity, is depicted by the dendrogram on the left side of the heatmap. As evident from the heatmap, a complex pattern of varying intensities is observed, suggesting the presence of differences or similarities among the samples and features being analyzed

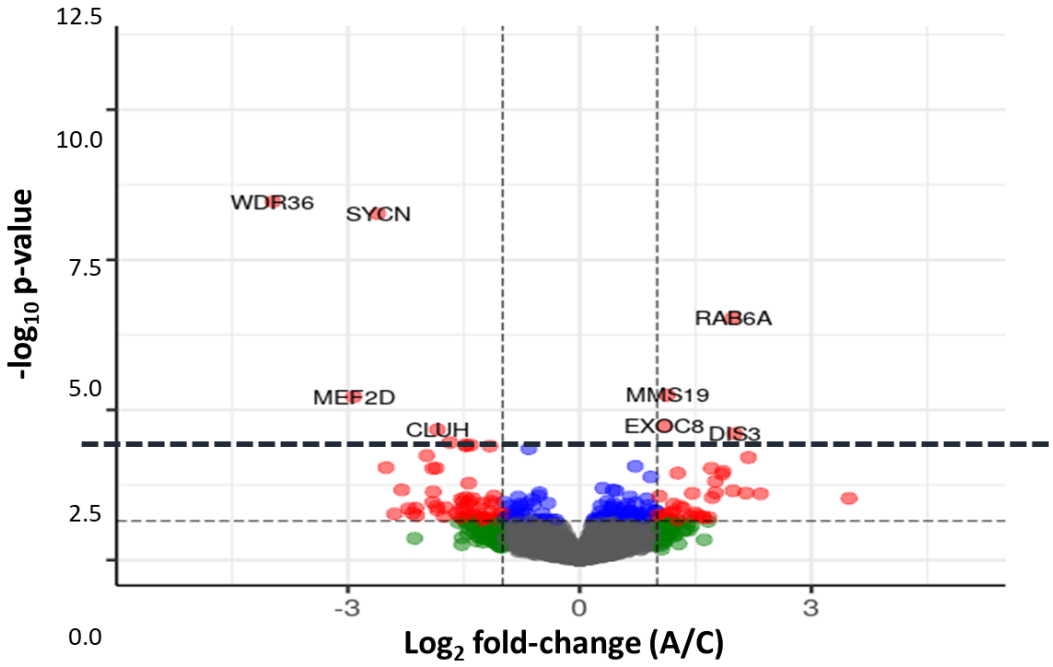

Figure 3. Differential protein expression analysis in aneurysm versus control groups via volcano plot. The volcano plot illustrates the differential expression of proteins between aneurysm (A) and control (C) groups from proteomic data. Log2 fold-change values (A/C) are plotted on the x-axis, indicating the magnitude of expression changes, while the negative log10 p-values are plotted on the y-axis, reflecting statistical significance. The horizontal dashed line represents the significance threshold for the p-values, while the vertical dashed lines indicate the fold-change expression cutoffs. Proteins falling outside these thresholds are considered differentially expressed. Statistically significant upregulated proteins in the aneurysm group include MMS19, EXOC8, DIS3 and RAB6a whereas key downregulated proteins comprise WDR36, SYCN, MEF2D, and CLUH.

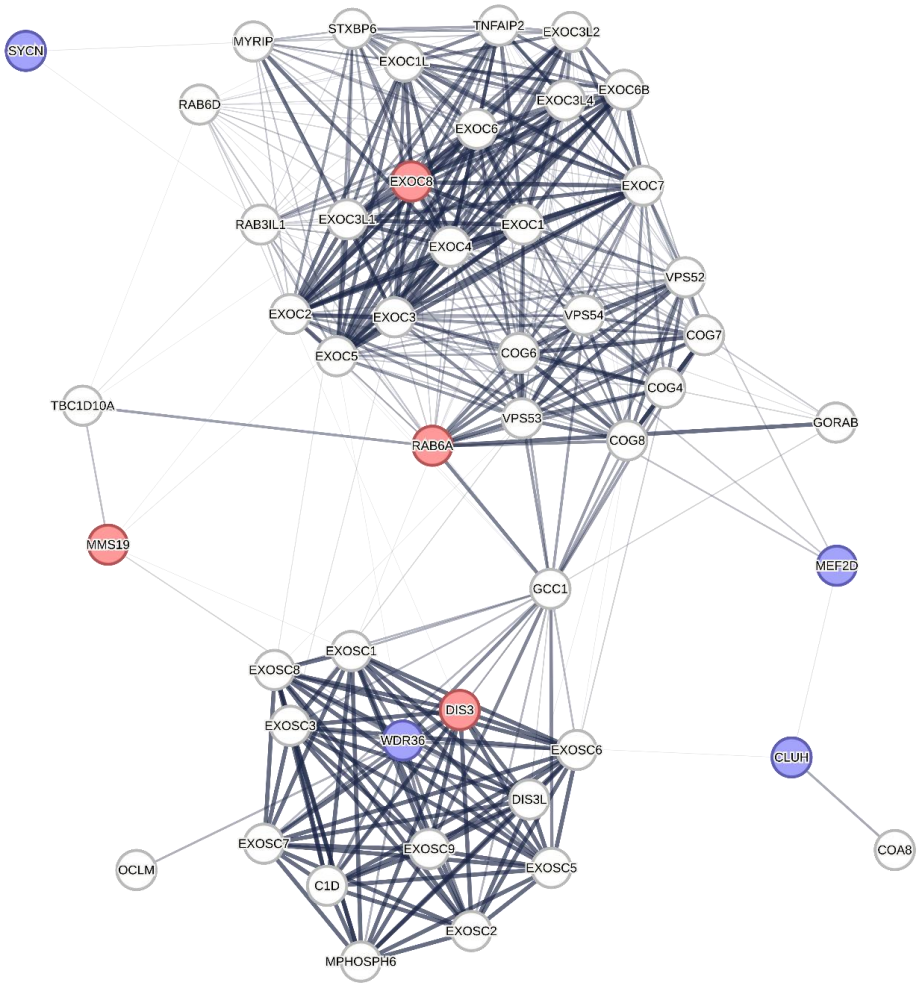

Figure 4. Protein-protein interaction network of up- and down-regulated proteins in the IA group compared to the control group. This network diagram represents the interactions among proteins that are differentially expressed in the IA group as compared to controls. Upregulated proteins are indicated with red nodes, including DIS3, EXOC8, RAB6A and MMS19, signifying their increased expression in IA. Downregulated proteins are shown with blue nodes, such as WDR36, SYCN, CLUHand MEF2D, representing their decreased expression. Nodes are connected by lines indicating known or predicted protein-protein interactions, with the thickness of the lines suggesting the strength of evidence supporting the interaction. The layout of the network highlights potential key regulatory proteins that may serve as central hubs in the pathogenesis of IA.

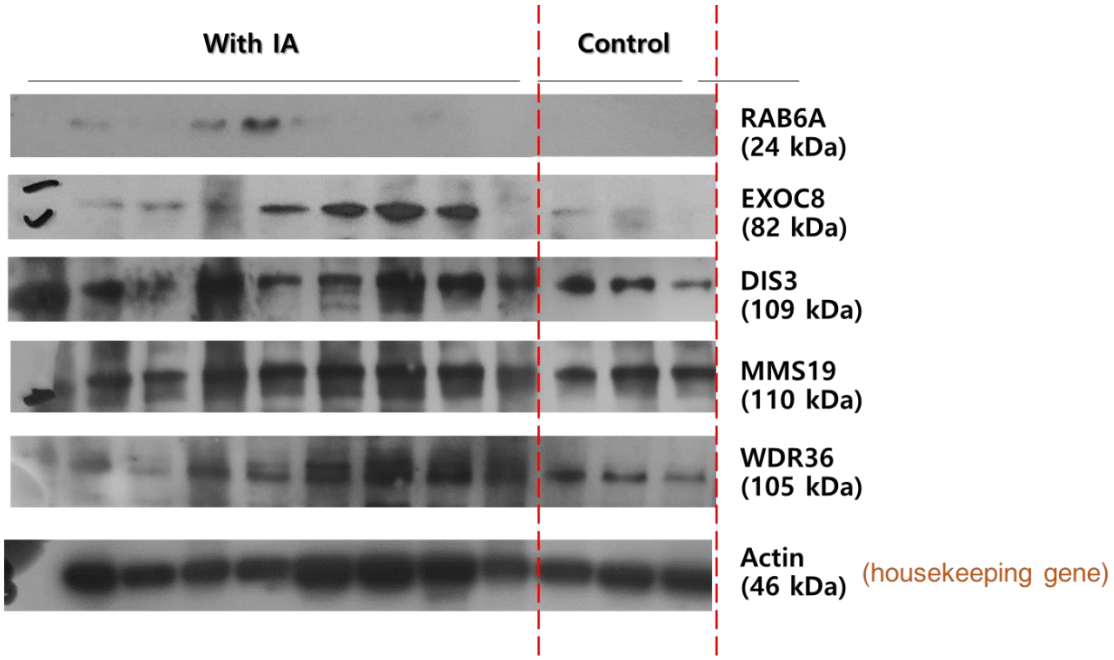

Figure 5. Western blot analysis displaying protein expression of candidate proteins in the study between the IA group and teh control group. The presence of the target proteins is indicated by the respective bands in the lanes. The housekeeping gene, Actin (46 kDa), is used as a loading control to ensure equal protein loading across all samples and serves as an internal control for normalization purposes.

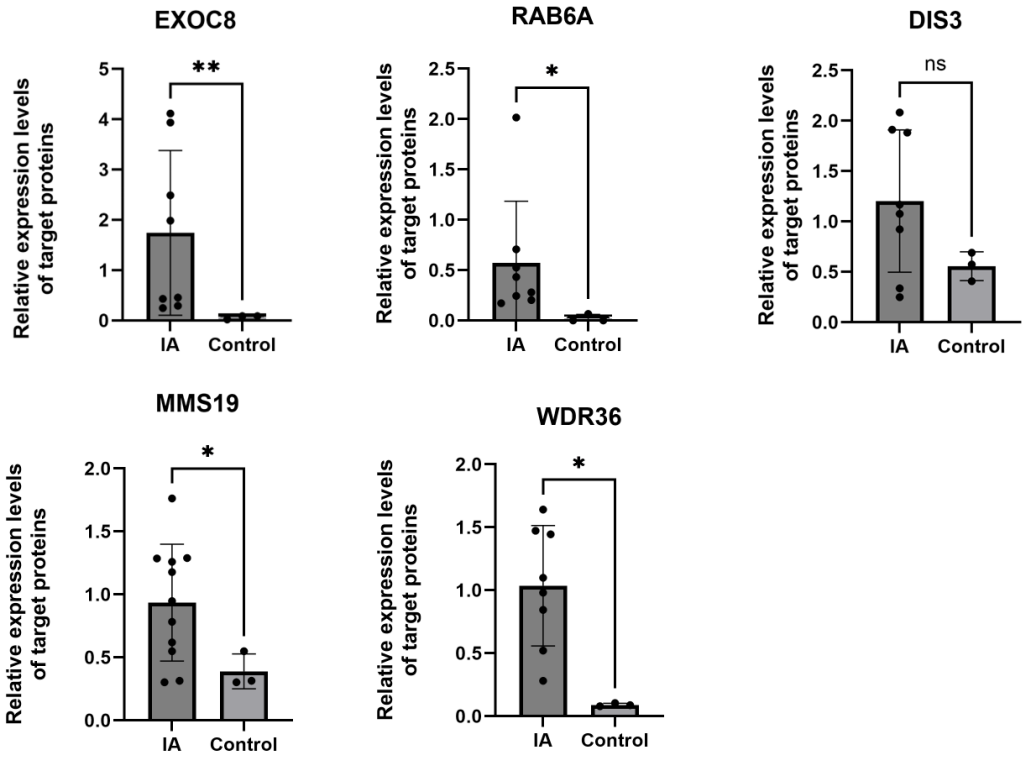

Figure 6. Relative expression levels of target proteins in ADPKD patients with and without intracranial aneurysms. The data are presented as mean expression levels with error bars representing the standard deviation. EXOC8 expression is significantly higher in the IA group than in the control group ($p < 0.01$). Similarly, RAB6A and MMS19 show significantly elevated expression levels in the IA group compared to the control group ($p < 0.05$ for both). No significant difference in DIS3 expression levels is observed between the two groups. WDR36 expression is also significantly higher in the IA group than in the control group ($p < 0.05$). Statistical significance is indicated by asterisks, with a single asterisk representing $p < 0.05$ and a double asterisk representing $p < 0.01$.

Supplementary data

Supplementary data 1. Description of the method used in whole exome sequencing

WES was performed following the CAP/CLIA validated standard operating protocol. Briefly, exome capture was performed using xGen Exome Research Panel v2 (Integrated DNA Technologies, Coralville, Iowa, USA) and sequencing was performed using the NovaSeqX platform (Illumina, San Diego, CA, USA) as 150bp paired-end reads. Sequencing data were aligned to the GRCh38 human reference genome using BWA-MEM and processed for variant calling by GATK v4.2.14. Variants were then annotated by Ensembl Variant Effect Predictor (VEP) and filtered and classified by EVIDENCE v4 following the American College of Medical Genetics and Genomics (ACMG) guideline. The filtered and classified variant list was manually reviewed by medical geneticists and physicians. The most likely variants that can explain the patient's phenotype were selected for reporting.

Supplementary figure 1.

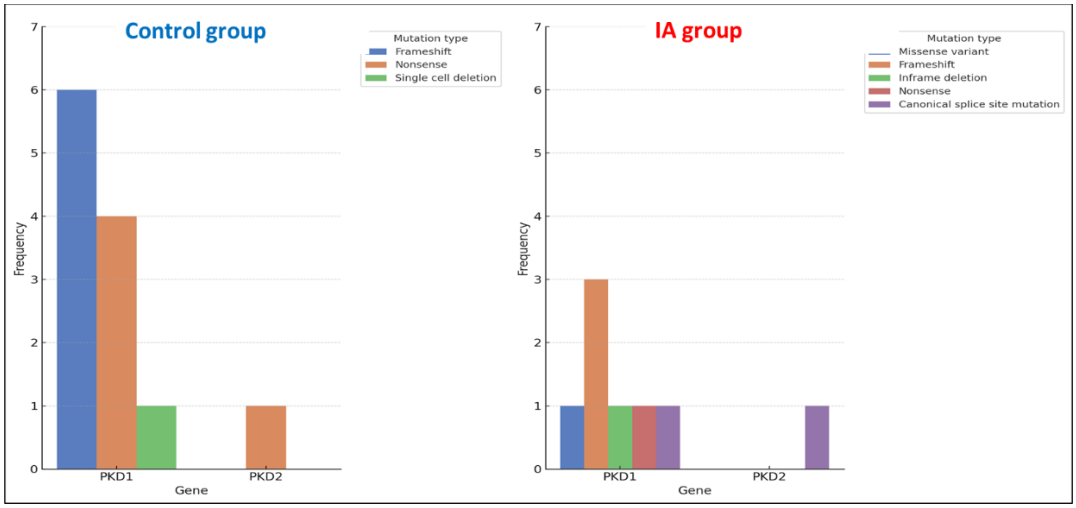

Figure S1. Frequency of mutation types in PKD1 and PKD2 genes across the groups. The bar graphs illustrate the distribution of different mutation types within each group. In the control group, frameshift and nonsense mutations are predominant in the PKD1 gene, with a single cell deletion also present. PKD2 mutations in the control group are all nonsense mutations. In the IA group, a diverse range of mutations is observed in the PKD1 gene, with the PKD2 gene showing only canonical splice site mutations.